



ELSEVIER

Available online at [www.sciencedirect.com](http://www.sciencedirect.com)

SCIENCE @ DIRECT®

**NIM B**  
Beam Interactions  
with Materials & Atoms

Nuclear Instruments and Methods in Physics Research B 223–224 (2004) 613–617

[www.elsevier.com/locate/nimb](http://www.elsevier.com/locate/nimb)

# Grain size distribution, $^{10}\text{Be}$ content and magnetic susceptibility of micrometer–nanometer loess materials

Chengde Shen <sup>a,\*</sup>, J. Beer <sup>b</sup>, P.W. Kubik <sup>c</sup>, M. Suter <sup>c</sup>, M. Borkovec <sup>d</sup>, T.S. Liu <sup>e</sup>

<sup>a</sup> Guangzhou Institute of Geochemistry, Chinese Academy of Sciences, Guangzhou, 510640, China

<sup>b</sup> Swiss Federal Institute of Environmental Science and Technology, EAWAG, CH-8600 Dübendorf, Switzerland

<sup>c</sup> Paul Scherrer Institute, c/o ETH-Hönggerberg, CH-8093 Zürich, Switzerland

<sup>d</sup> Institute of Terrestrial Ecology, c/o ETH, CH-8092 Zürich, Switzerland

<sup>e</sup> Geology and Geophysics Institute, Chinese Academy of Science, Beijing 100029, China

## Abstract

Grain size distribution,  $^{10}\text{Be}$  content and magnetic susceptibility of loess particles in the Luochuan section were measured and the results are discussed in terms of fragmentation and fractal theory. The fact that the order of increasing specific surface area of bulk samples from the horizons of  $S_0$ ,  $L_1LL_1$ ,  $L_1LL_2$ ,  $S_1$  and  $L_2$  is consistent with the order of successively warmer palaeo-climate may provide a new indicator for palaeo-climatic and palaeo-environmental studies. The values of fractal dimension for the grains of  $S_1$  and  $L_2$  are 2.80 and 2.76, respectively. Our results also show that the magnetic properties of loess particles depend strongly not only upon particle size but also upon pedogenic characteristics and that  $^{10}\text{Be}$  is mainly adsorbed on the surface of ultra-fine particles, independent of pedogenic process.

© 2004 Elsevier B.V. All rights reserved.

PACS: 91.65.Br; 91.65.Dt; 91.25.Ng

Keywords: Loess; Nanometer grains; Fractal theory;  $^{10}\text{Be}$ ; Magnetic susceptibility

## 1. Introduction

Loess material, as an aeolian deposit, is characterized by a correlation between its size distribution and palaeo-climatic and palaeo-environmental parameters such as the wind-field, rainfall and humidity in the past [1–5]. A number of studies are now available [1,6,7] about  $^{10}\text{Be}$  and magnetic mineralogy in loess as a function of

particle size. These studies clearly show that the behavior of  $^{10}\text{Be}$  in loess profiles depend on the particle properties rather than on the chemistry and that the magnetic signal is mainly recorded in particles less than 1  $\mu\text{m}$  in size. Based on  $^{10}\text{Be}$  and magnetic measurements on loess material the annual mean rainfall was estimated for the last 150 000 years [8]. However, due to difficulties in separation of ultra-fine particles so far no effort has been made to extend these studies to the sub-micrometer range. In this paper, the successful separation of ultra-fine particles from Luochuan loess (palaeosol  $S_1$  and loess  $L_2$ ) and the analysis of micrometer–nanometer particles regarding size,

\* Corresponding author. Tel.: +86-20-8529-0062; fax: +86-20-8529-0130.

E-mail address: [cdshen@gig.ac.cn](mailto:cdshen@gig.ac.cn) (C. Shen).

susceptibility and  $^{10}\text{Be}$  concentrations are discussed. These results should provide some insight into the pedogenic processes contributing to the origin of magnetism susceptibility and the geochemistry of  $^{10}\text{Be}$ .

## 2. Experimental

In Fig. 1, the stratigraphy and the sampling layers for horizons of  $S_0$ ,  $L_1LL_1$ ,  $L_1LL_2$ ,  $S_1$ ,  $L_2$  are shown. The two samples from palaeosol  $S_1$  and loess  $L_2$  were divided into ten size ranges. The  $>50$ , 40, 20, 10 and 3  $\mu\text{m}$  ranges were separated by normal sieving and those of 0.9 and 0.3  $\mu\text{m}$  and 90, 30 and 10 nm ranges by centrifugation. Particles in the micrometer–nanometer range were examined

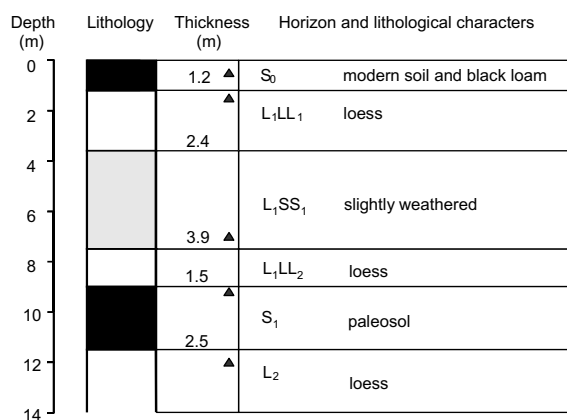


Fig. 1. The stratigraphy in the uppermost part of the loess section at Luochuan in the central Chinese loess plateau. Palaeosols ( $S_0$ ,  $S_1$ ) are shaded dark, unweathered loess ( $L_1LL_1$ ,  $L_1LL_2$ ,  $L_2$ ) are white, slightly weathered loess ( $L_1SS_1$ ) is light grey. Loess layers are mainly formed by northerly winter monsoons, whereas palaeosols are subject to relatively strong pedogenesis related to strong summer monsoons carrying more moisture and less dust. (▲) Sampling layer.

using sieving, sedimentation, small angle static light scattering, centrifugation, dynamic light scattering, respectively. Surface areas of particles in all the size ranges were determined by the nitrogen-absorption technique [9].

To extract the  $^{10}\text{Be}$  each sample was leached with 20 ml of 6 M HCl for 24 h. The solution was separated from the residue by centrifuging. Then a second leaching was performed. The two solutions were combined and heated to dryness under a hot lamp. Beryllium and aluminum was alternately precipitated and redissolved by varying the pH between 8 and 15. Aluminum was separated by masking it with EDTA. Finally,  $\text{Be}(\text{OH})_2$  was oxidized to  $\text{BeO}$ , mixed with copper powder and pressed into a copper disc for use in the ion source of the accelerator mass spectrometer [1]. All  $^{10}\text{Be}$  measurements were carried out using the ETH/PSI accelerator mass spectrometer at Zürich. The  $^{10}\text{Be}/^9\text{Be}$  ratio of the blanks were typically  $10^{-14}$ , whereas the  $^{10}\text{Be}/^9\text{Be}$  ratio of the sample were typically  $10^{-12}$ . Each sample was measured at least twice, resulting in an accuracy ( $1\sigma$ ) 3–5% [10].

All grain separation and size measurements were completed at the Institute of Terrestrial Ecology of the ETH. The magnetic susceptibility was determined using the Bartington susceptibility meter of the Institute of Geophysics of the ETH Zürich.

## 3. Results

Specific surface area,  $^{10}\text{Be}$  and magnetic susceptibility measurements for bulk samples of loess and palaeosol are given in Table 1. Specific surface area,  $^{10}\text{Be}$  and Magnetic susceptibility and the fractional mass  $^{10}\text{Be}$  and susceptibility of  $S_1$  palaeosol and  $L_2$  loess in different size ranges are given in Tables 2 and 3, respectively.

Table 1  
Specific area,  $^{10}\text{Be}$  and magnetic susceptibility of bulk samples of loess and palaeosol

Horizon	$S_0$	$L_1LL_1$	$L_1LL_2$	$S_1$	$L_2$
Specific area ( $\text{m}^2/\text{g}$ )	14.64	12.27	14.31	20.34	13.92
$^{10}\text{Be}$ ( $10^8$ atoms/g)	3.49	2.32	3.50	4.03	2.81
Magnetic susceptibility ( $10^{-7}$ $\text{m}^3/\text{kg}$ )	16.18	5.47	5.93	22.8	4.93

Table 2

Specific area,  $^{10}\text{Be}$  and magnetic susceptibility of  $S_1$  palaeosol and  $L_2$  loess particles in different size ranges

Grain size	>50 $\mu\text{m}$	40 $\mu\text{m}$	20 $\mu\text{m}$	10 $\mu\text{m}$	3 $\mu\text{m}$	900 nm	300 nm	90 nm	30 nm	10 nm
$S_1$ -SA ( $\text{m}^2/\text{g}$ )	2.15	2.00	2.41	4.80	13.15	34.46	53.50	68.83	–	–
$L_2$ -SA ( $\text{m}^2/\text{g}$ )	1.42	2.60	3.51	6.04	14.03	42.15	62.47	–	–	–
$S_1$ - $^{10}\text{Be}$ ( $10^8$ atoms/g)	0.70	0.95	1.40	2.80	5.80	7.40	8.10	9.46	8.60	7.90
$L_2$ - $^{10}\text{Be}$ ( $10^8$ atoms/g)	1.25	0.95	1.40	2.05	3.30	3.95	3.49	3.53	4.59	1.97
$S_1$ -MS ( $10^{-7}$ $\text{m}^3/\text{kg}$ )	2.38	6.63	8.53	11.82	26.40	44.14	59.14	70.89	59.58	10.19
$L_2$ -MS ( $10^{-7}$ $\text{m}^3/\text{kg}$ )	1.16	3.84	4.02	4.89	6.63	8.13	9.38	11.96	11.95	4.55

SA: specific area; MS: magnetic susceptibility.

Table 3

Fractional mass,  $^{10}\text{Be}$  and magnetic susceptibility of  $S_1$  palaeosol particles in different size ranges

Grain size	>50 $\mu\text{m}$	40 $\mu\text{m}$	20 $\mu\text{m}$	10 $\mu\text{m}$	3 $\mu\text{m}$	900 nm	300 nm	90 nm	30 nm	10 nm
Fractional mass (%)	6.0	30	12.4	17.7	11.8	11.2	5.0	4.34	2.28	0.86
$^{10}\text{Be}$ ( $10^8$ atoms/g)	0.70	0.95	1.40	2.80	5.80	7.40	8.10	9.46	8.60	7.90
F- $^{10}\text{Be}$ ( $10^8$ atoms/g)	0.04	0.29	0.17	0.50	0.68	0.83	0.41	0.41	0.20	0.07
MS ( $10^{-7}$ $\text{m}^3/\text{kg}$ )	2.38	6.63	8.53	11.82	26.40	44.14	59.14	70.89	59.58	10.19
F-MS ( $10^{-7}$ $\text{m}^3/\text{kg}$ )	0.14	1.99	1.06	2.09	3.12	4.94	2.96	3.08	1.36	0.09

F: fractional mass; MS: magnetic susceptibility; F- $^{10}\text{Be}$ : fractional  $^{10}\text{Be}$  concentration; F-MS: fractional magnetic susceptibility.

## 4. Discussion

### 4.1. Characteristics of size distribution in loess material

Loess formation and pedogenesis are very complex nonlinear processes and to interpret the size distribution of loess material we use a fragmentation model. The model describes the starting and the development of the fragmentation process as well as their inter-relationship. The relationship between the number and the size of fragments can be described by the fractal theory [11,12],  $N(r) \propto r^{-D}$ , where  $N(r)$  stands for the number of particles larger than  $r$  in radius per unit volume;  $D$ , as the fractal dimension, which gives information about the extent of fragmentation.

The size distribution data of  $S_1$  palaeosols in Luochuan section are plotted in a  $\log n(r)$  versus  $\log r$  diagram (Fig. 2) where  $n(r)$  refers to the number density of particles per unit volume. By fitting the data points according to the relationship

$$n(r) = \frac{-dN(r)}{dr} \propto r^{-D-1}, \quad (1)$$

a  $D$  value of  $2.80 \pm 0.1$  can be obtained. By analogy, the  $L_2$  loess gives  $D = 2.76 \pm 0.07$ . However,

apparent deviations from  $D = 2.80$  can be noticed in both the large and the small extremes over the size range in Fig. 2. Particles smaller than 10 nm in size show a smaller slope, indicating that the total number of particle does not increase infinitely with increasing division. On the other hand, a steeper slope is recognized in the 10–100  $\mu\text{m}$  range, indicating that an upper limit of particle size exists and thus the integrated mass density [ $\propto r^3 n(r)$ ] is meaningful. Based on Fig. 2, the particle size of  $S_1$  palaeosol has a lower limit of 10–50 nm and an upper limit of 10–100  $\mu\text{m}$ . The distribution of particle size obeys a power law with the exponent  $D = 2.80$ . These results prove that the present experimental procedures for ultra-fine particles separation are successful.

### 4.2. Specific area, $^{10}\text{Be}$ and magnetic susceptibility of bulk samples

Specific areas together with  $^{10}\text{Be}$  and magnetic susceptibility were measured for bulk samples from horizons  $S_0$ ,  $L_1LL_1$ ,  $L_1LL_2$ ,  $S_1$ ,  $L_2$  and the results are listed in Table 1. As can be seen, the order of increasing specific area for these samples,  $L_1LL_1$ – $L_2$ – $L_1LL_2$ – $S_0$ – $S_1$  (e.g. loess–black loam–palaeosol), reflects just the trend of increasingly

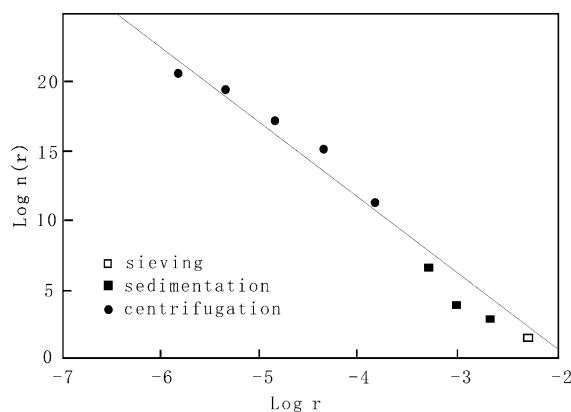


Fig. 2. Number density of micrometer–nanometer range particles in palaeosol  $S_1$ , Luochuan section, as a function of radius. Particles separated by sieving ( $\square$ ), sedimentation ( $\blacksquare$ ) and centrifugation ( $\bullet$ ).  $r$ : the particle radius (cm);  $n(r)$ : the measured number distribution density ( $\text{cm}^{-4}$ ).

warmer palaeo-climate and promising to be a potential indicator of palaeo-climate and palaeo-environment. A good correlation between specific area and  $^{10}\text{Be}$ , magnetic susceptibility shows that  $^{10}\text{Be}$  is attached to the surface of the particles and magnetic susceptibility mainly exists in the fine ferromagnetic material particles some of which are produced during pedogenic processes [2,8].

The significantly larger specific area of palaeosols than those of loess suggests that the palaeosol is made up of finer grains with rougher surfaces as a result of chemical and organic weathering during pedogenesis. However, as shown in Table 2, loess has larger specific area than palaeosol with respect to the same size range except for those  $>50\ \mu\text{m}$ . This is thought to be probably due to a higher degree of original roughness in the former. Particles of  $L_2$  may have preserved to a large extent their irregular shape before transport while particles in  $S_1$  may have rounded by later weathering. Further studies are warranted in this respect to establish an alternative palaeo-climatic and palaeo-environmental indicator.

#### 4.3. Variations of $^{10}\text{Be}$ and magnetic susceptibility with grain size

$^{10}\text{Be}$  and magnetic susceptibility of particles in the  $50\ \mu\text{m}$ – $10\ \text{nm}$  range in  $S_1$  and  $L_2$  are shown in

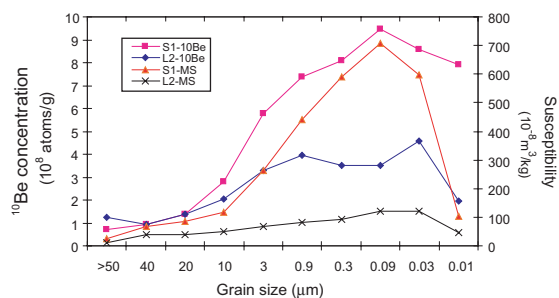


Fig. 3.  $^{10}\text{Be}$  and magnetic susceptibility of micrometer–nanometer range particles from  $S_1$  palaeosol and  $L_2$  loess, Luochuan section, as a function of grain size. MS = magnetic susceptibility.

Table 2 and Fig. 3. The fractional mass,  $^{10}\text{Be}$  and susceptibility of  $S_1$  palaeosol particles in different size ranges are shown in Table 3. As can be seen from Table 2 and Fig. 3: (1) Palaeosol magnetic susceptibility varies from 23.8 to 709 ( $10^{-8}\ \text{m}^3/\text{kg}$ ) with a “sharp peak value” between 30 and 900 nm, while little variation has been found in loess without any “peak value” at all; (2) In size ranges larger than  $10\ \mu\text{m}$  and smaller than 30 nm, very low magnetic susceptibility is noticed in either loess or palaeosol, suggesting the dominance of non-magnetic material in these size ranges. These observations indicate that susceptibility is apparently size-dependent and is closely related to pedogenic process. In Fig. 3, the  $^{10}\text{Be}$  content and the magnetic susceptibility show a similar profile, and the increase of the  $^{10}\text{Be}$  content with decreasing particle size is not monotonous. Moreover, one can easily find the decrease tendency of the  $^{10}\text{Be}$  content in the finest (10 nm) particles for  $L_2$  and  $S_1$ . A possible explanation is  $^{10}\text{Be}$  not related to the process of pedogenesis.

From Table 1, we can find that the values of magnetic susceptibility of bulk palaeosol  $S_1$  and loess  $L_2$  are  $228 \times 10^{-8}$  and  $49.3 \times 10^{-8}\ \text{m}^3/\text{kg}$ , respectively. Obviously, the former is 4.6 times as much as the latter. Based on fractional mass (%) and mass susceptibility of grain size particles, the susceptibility of fractional mass can be obtained (Table 3), which indicates a proportion of total mass susceptibility in bulk sample to the magnetic susceptibility of fractional mass. By analogy, the  $^{10}\text{Be}$  concentration of fractional mass can be also

obtained (Table 3). The integrated values of magnetic susceptibility of fractional mass (F-MS) of  $S_1$  and  $L_2$  are  $208 \times 10^{-8}$  and  $50.7 \times 10^{-8}$  m<sup>3</sup>/kg, respectively, which are consistent with the magnetic susceptibility values of bulk samples of palaeosol  $S_1$  and loess  $L_2$  shown in Table 1. Obviously, the separation experiments of ultra-fine particles in this work are successful.

## 5. Conclusions

(1) Particles in 10 nm size range can be successfully separated by centrifugation from loess and palaeosol samples.

(2) The sequence of increasing surface area in bulk samples from the horizons is consistent with their palaeo-climatic trend from cold to warm. The specific surface area is therefore a potential indicator of ancient climate and environmental conditions. The values of fractal dimension for the grains of  $S_1$  and  $L_2$  are 2.80 and 2.76, respectively.

(3) Apparently magnetic susceptibility of loess material in the micrometer–nanometer range can be correlated to particle size and to the characteristics of pedogenic processes. <sup>10</sup>Be is mainly adsorbed on the surface of ultra-fine particles and no relation can be established between its concentration and the process of pedogenesis.

## Acknowledgements

We thank the AMS group ETH for their contributions during <sup>10</sup>Be measurements. The <sup>10</sup>Be

measurements were performed at the AMS-facilities, jointly operated by the Swiss Federal Institute of Technology, Zürich and Paul Scherrer Institut, Villigen, Switzerland. This work was supported jointly by grants from Chinese NKBRF (G1999043401), CAS Knowledge Innovation Project (KZCX2-SW-118, KZCX2-108), NSFC (40231015) and also from the Swiss NSF, ETH Zürich, the Paul Scherrer Institute. We are also grateful for the constructive comments of two anonymous reviewers.

## References

- [1] C.D. Shen, J. Beer, T.S. Liu, H. Oeschger, G. Bonani, M. Suter, W. Wölfli, *Earth Planet. Sci. Lett.* 109 (1992) 169.
- [2] B.A. Maher, *Phys. Earth Planet. Interior.* 42 (1986) 76.
- [3] B.A. Maher, R. Thompson, *Quatern. Res.* 37 (1992) 155.
- [4] H.B. Zheng, F. Oldfield, L.Z. Yu, J. Shaw, *Z.S. An, Phys. Earth Planet. Interior.* 68 (1991) 250.
- [5] X.M. Liu, J. Shaw, T.S. Liu, F. Heller, B.Y. Yuan, *Geophys. J. Int.* 108 (1992) 301.
- [6] C. Shen, J. Beer, F. Heller, P.W. Kubic, M. Suter, T. Liu, *Nucl. Instr. and Meth. B* 172 (2000) 551.
- [7] J. Beer, C.D. Shen, F. Heller, T.S. Liu, G. Bonani, B. Ditttrich, M. Suter, *Geophys. Res. Lett.* 20 (1993) 57.
- [8] F. Heller, C.D. Shen, J. Beer, X.M. Liu, T.S. Liu, A. Bronger, M. Suter, G. Bonani, *Earth Planet. Sci. Lett.* 114 (1993) 385.
- [9] S.J. Gregg, K.S.W. Sing, *Adsorption, Surface Area and Porosity*, Academic Press, 1982.
- [10] M. Suter, R. Balzer, G. Bonani, H. Hofmann, E. Morenzon, M. Nesi, W. Wölfli, M. Andree, J. Beer, H. Oeschger, *Nucl. Instr. and Meth. B* 233 (5) (1984) 117.
- [11] D.L. Turcotte, *J. Geophys. Res. B* 91 (2) (1986) 1921.
- [12] M. Borkovec, Q. Wu, G. Degovics, P. Laggner, H. Sticher, *Colloids and Surf. A: Phys. Eng. Aspect* 73 (1993) 65.